

## Aerodynamic Characteristics of a Rectangular Wing Using Non-Linear Vortex Ring Method

Anmar Hamid Ali

Lecturer

Engineering College-Baghdad University

aha\_has@yahoo.com

### ABSTRACT

The aerodynamic characteristics of general three-dimensional rectangular wings are considered using non-linear interaction between two-dimensional viscous-inviscid panel method and vortex ring method. The potential flow of a two-dimensional airfoil by the pioneering **Hess & Smith** method was used with viscous laminar, transition and turbulent boundary layer to solve flow about complex configuration of airfoils including stalling effect. Viterna method was used to extend the aerodynamic characteristics of the specified airfoil to high angles of attacks. A modified vortex ring method was used to find the circulation values along span wise direction of the wing and then interacted with sectional circulation obtained by **Kutta-Joukowski** theorem of the airfoil. The method is simple and based mainly on iterative procedure to find the wings post stall aerodynamic results. Parametric investigation was considered to give the best performance and results for the rectangular wings. Wing of NACA 0012 cross sectional airfoil was studied and compared with published experimental data for different speeds and angle of attacks. Pressure, skin friction, lift, drag, and pitching moment coefficients are presented and compared good with experimental data. The present method shows simple, quick and accurate results for rectangular wings of different cross-section airfoils.

**Key words:** lifting line method, Viterna method, potential flow, viscous-inviscid panel method

### خصائص الديناميكا الهوائية لجناح مستطيل باستخدام طريقة الدوامة الحلقية غير الخطية

انمارحامد علي

مدرس

كلية الهندسة – جامعة بغداد

#### الخلاصة

تمت دراسة الخصائص الايروديناميكية للاجنحة الثلاثية الابعاد المستطيلة الشكل باستخدام التأثير اللاخطي المتبادل بين طريقة الالواح لزوج-غير لزوج ثنائية البعد وطريقة الدوامة الحلقية. ان الجريان الكامن لجنيح ثنائي البعد بطريقة Hess و Smith البدائية قد استخدم مع الطبقة المتاخمة الطباقية، الانتقالية والمضطربة لحل الجريان حول اشكال معقدة من الجنيحات متضمنا تأثير الانهواء فيها. طريقة فيتيرنا استخدمت لتمديد الخواص الايروديناميكية للجنيح الى زوايا هجوم عالية. طريقة الدوامة الحلقية المعدلة استخدمت لاجاد قيم التدوير على طول امتداد الجناح واجاد تأثيرها مع التدوير المقطعي الماخوذة من نظرية **Kutta-Joukowski** للجنيح. الطريقة بسيطة وتعتمد اساسا على عملية التأثير المتبادل لاجاد النتائج الايروديناميكية الاجنحة ما بعد الانهواء. تمت دراسة العوامل التي تعمل على اعطاء افضل اداء ونتائج للمسالة. الجناح ذو مقطع مطيار NACA 0012 تمت دراسته ومقارنته مع البيانات العملية المنشورة لمختلف السرع وزوايا الهجوم. معامل الضغط، الاحتكاك، الرفع، الممانعة، و عزم التارجح قد تم عرضها ومقارنتها جيدا مع البيانات العملية. ان الطريقة الحالية تظهر بساطة، سرعة ودقة النتائج للجناح المستطيل ولمختلف مقاطع الجنيحات.

## 1. INTRODUCTION

The conceptual design of aircraft requires numerous representative calculations to a large number of aircraft configurations. Fast methods to find the aerodynamic characteristics have been of great interest. The Navier-Stokes equations results are too complex calculations during aircraft design phase, in other hand Lifting line, vortex lattice and panel methods are still used today as a tool to find the aerodynamic characteristics of aircrafts. The potential methods have the same assumptions irrotational, incompressible and discretization at the wing and body of the aircraft. These methods are simple, fast, and need small computer memory to solve them.

In lifting line and vortex methods, the airfoil shape is not a part of solution and this may cause errors when calculating the configurations have un-conventional airfoils. These errors could be obtained due to the assumption of no stalling characteristics, and then no profile drag could be estimated (only induced drag). Moderate to high angle of attacks during take-off, landing and military aircraft manoeuvring have inclusion of non-linear aerodynamic characteristics. Accurate predictions of the flow in those conditions are needed during design phases especially in structure modelling.

Two-dimensional airfoil data lift, drag and pitching moment are available from the experimental, Navier-Stokes solutions and even by panel method interacted with boundary layer solution as in **Eppler, and Somers, 1980, Drela, 1989, and Ali, 2014**. Various methods were available to solve two-dimensional airfoil sectional characteristics (lift, drag and pitching moment) which used as input data to calculate three-dimensional aerodynamic characteristics of wings. The solution is simple, fast and less hardware demanding as compared with CFD computations.

An early method was presented in **Sivells, and Neely, 1947**; the local lift coefficient for NACA 4-series airfoil was interacted with lifting-line method. The vortex strengths along the span of a wing were solved using iteration method. The induced drag with final span wise circulation distribution were presented and discussed with previous experimental works. The drawback of the method is the limitation of lifting line method for large aspect ratio and small swept wings. A two-dimensional steady incompressible flow was calculated for NASA GA(W)-1 airfoil characteristics using linear vortex panel method interacted with boundary layer laminar, transition and turbulent regions for attached and separated flow had been presented in **Piszkin and Levinsky, 1976**. Lifting line method was used to calculate flow in three-dimensional wing using the characteristics of two-dimensional airfoil lift curve. Only distributed load and wake shape of the rectangular wing were showed.

Dropped and un-dropped leading edge wing in post stalling region were studied by **Anderson, et al., 1980**, to find non-linear post stall behaviour of a rectangular wing. Experimental airfoil characteristics of dropped and un-dropped shape were incorporated with prandtle lifting line method to solve the problem. The accuracy of the results was 20% as compared with the experimental works. No pressure or shear stresses distribution presented in the work.

The quick aerodynamic characteristics predictions for high lift module during conceptual design stages of an aircraft was made by coupling a non-linear lifting surface method (modified **Weissinger** method) with two-dimensional viscous characteristics of aircraft to calculate three-dimensional wing of the designed aircraft was presented in **Van Dam, et al., 2001**. Semi-empirical equations for two-dimensional high lift airfoils were utilized based on the computational fluid dynamic (CFD) and experimental data for different configurations. The method provided necessary accuracy and fast enough for the design stage.

Multiple wings aerodynamic characteristics prediction method for post stall flight condition was shown in **Mukherjee, and Gopalarathnam, 2003**. De-cambering approach was developed in each section of wing to consider viscous effect at high angle of attack. The results were presented to lift coefficient as a function of angle of attack and load distribution along span wise direction of the aircraft.

Different approaches were used to find the interaction between potential solution and two-dimensional viscous effects at high angle of attack. Most of the models were developed based on the two-dimensional lift-angle of attack curve at moderate to high ranges experimentally as shown in **de Vargas, and de Oliveira, 2006, Pakalnis, Lasauskas, and Stankunas, 2005, and Spalart, 2014**.

The most important notes about all the previous considerations are that, the presented results were restricted to lift, drag coefficients and load distribution along span wise direction of the wing of the aircraft only. This may be attributed to the information used as input (two-dimensional airfoil lift and drag curves) to solve the characteristics of the wing. The pressure and boundary layer characteristics distributions along upper and lower surfaces were not consisted in the results. So that, in the present work the aerodynamic characteristics with pressure and boundary layer parameters will be studied and demonstrated using vortex ring method which was discussed in **Ali, 2010** to solve the potential linear behaviour of a rectangular wing and then coupled with the two-dimensional viscous-inviscid interaction method of multi-element airfoil in ground effects illustrated by **Ali, 2014**. Viterna method **Tangler, and Kocurek, 2005** was used to extrapolation the lift and drag forces of the wing sectional airfoil without need for extra solution of a large angle of attacks. Iteration method will be used to find the circulations along the span wise direction of rectangular wings.

The presentation of a non-linear vortex ring method will be discussed in theory of the method section, which illustrates the iterative procedure used to include airfoil distribution characteristics data to the wing calculation of circulation distribution along span wise direction and the results are discussed. Parametric investigation and results verification are done by comparing with the experimental published data. Last conclusions and future work are stated.

## 2. THEORY OF THE METHOD

For small to moderate angles of attack, linear aerodynamic characteristics can be modelled for most aircrafts wings, but at high angles of attack a non-linear behaviour of forces and moment are produced. Panel methods are linear solution, so it cannot take into account the non-linearity of the stall effects. In the present method the non-linearity effects of un-swept to moderate swept wings the vortex ring method of **Ali, 2010** is modified to account the stalling effects.

### 2.1 Two Dimensional Airfoil Characteristics

A general method for inviscid-viscous boundary layer interaction method is used to calculate flow about multi-element airfoil in ground effect which was described in details by **Ali, 2014**. Two-dimensional **Hess, and Smith, 1967** panel method with constant source and vortex distribution is used to find the potential flow around complex configurations of multi-elements airfoils like slats and flaps high lift elements. Each elements of the configuration are discretized using flat panels on the upper and lower side of the airfoil. Constant source strength is assumed

at control point of the panel with constant vortex strength for the whole airfoil. Boundary condition of zero normal velocity is applied at the control points with Kutta condition at the trailing edge of the airfoil. The linear equations which are obtained from influence each panel by the other are solved to determine the unknown strengths of the main airfoil and its elements. The boundary layer growths along the upper and lower sides of multi-element airfoils are calculated by using the pressure and velocity of the potential flow which were solved previously. The boundary layer regions are solved by using the method of **Thwait's** for laminar flow,  $n^9$ - or **Micheal's** methods for transition point and **Head's** method for turbulent flow along upper and lower surfaces of the airfoil. Iterative scheme with transpiration method is used for each control point to investigate the viscous effect in the boundary condition of panel method of the airfoil. Ground effect is considered by imaging the configuration around ground x-axis. Wake shape is relaxed optionally to give more realism to the calculations.

Direct and inverse methods are used to calculate linear and non-linear (separating flow) behaviour of the aerodynamic characteristics around MEA in ground effects. The program is presented and discussed for different cases and tested in **Ali, 2014**. Comparisons were showed good agreement between the theoretical and experimental results for low to moderate angles of attack.

Non-linear behaviour characteristics of an airfoil can be obtained for small to moderate angles of attack by using previous method, but at higher angles or even in negative angles of attack the convergence is not reached. Viterna method **Tangler**, and **Kocurek, 2005**, was developed to extrapolate lift and drag coefficients to extreme angles using flat plate theory and empirical assumptions obtained from experimental data for losses in BEM. In present method, the forces and moments are evaluated through Viterna method for post stall angles, but pressure and boundary layer properties are restricted to the method of interaction presented previously. Single element airfoil is considered in the present analysis.

## 2.2 Three Dimensional Wing Characteristics

In a vortex ring method, a non-planar finite wing is discretized into number of sections where for each section only one quadrilateral panel in chord wise directions is represented. A vortex ring shape placed at quarter chord line for each panel to satisfy the boundary condition of zero normal velocity of the wing using Biot-Savart law of vorticity. The wake behind the wing is discretized using single long element (about 2-3 times span length **Katz**, and **Plotkin, 1991**) or multiple elements along wake length (optionally to calculate wake shape effects) for each section as shown in **Fig. 1**. The two-dimensional discretization of the cross-sectional airfoil geometry into finite number of element in a clockwise direction beginning from the trailing edge lower surface to the upper surface trailing edge and in span wise direction to form the surface elements are shown in **Fig. 2**. Kutta condition at the trailing edge is used to calculate the strengths of the wake elements. The flow tangency boundary condition is satisfied at three-quarter chord point for each panel (centre point of the vortex ring). Linear sets of influence coefficients equations are solved using Gauss's elimination method to find the strengths of vortices of the panels. Optionally the wake may be relaxed to be a stream line starting from the trailing edge. Different test cases are presented and discussed in **Ali, 2014**. The wing discretization in the present study is limited to one element in the chord wise direction because the final circulation distribution of the wing will be related to the sectional two-dimensional airfoil characteristics calculated previously. The potential solution of rectangular wing using vortex ring method for different angle of attack and aspect ratio will be showed and discussed in the results section.

### 2.3 Method of interaction

The extension of the linear potential vortex ring method to the non-linear viscous post stalling characteristics at high angle of attack is presented in this section. Kutta-Joukowski theorem of lift is the main idea of this method. The sectional circulation of the wing (vortex strength at each section of wing by using vortex ring method) is related to the circulation obtained from two-dimensional airfoil data which was investigated and stored for each section. The induced angle of attack is calculated at each section from vortex ring method at load points (centre point of bound vortex segment). The induced angle simply represents the angle between the down wash velocities divided by free stream velocity. The effective angle of attack is then evaluated by subtracting induced angle from geometrical angle of attack at each section. Two-dimensional airfoil lift coefficient is evaluated at the effective angle of attack of each section. The circulations for three- and two-dimensional analysis are compared and damped by using iterative procedure to find new value. The following steps are used to calculate the non-linear vortex ring method,

- 1- Geometric and operational conditions parameters are defined starting from root to tip which consists of (airfoil geometric coordinates, tip coordinates of the wing, chord length, geometric angle of attack, number of span wise sections, wake options for root and tip sections).
- 2- Two-dimensional airfoil aerodynamic characteristics are calculated for the root and tip airfoils by using viscous-inviscid interaction method of the multi-element airfoil in ground effects for angle of attack range (-10 to 20°) as discussed in the section 2.1.
- 3- Viterna method is used to extrapolate the airfoil characteristics (lift and drag coefficient) to extreme ranges of angles of attack as discussed in the section 2.1.
- 4- The airfoil results (pressure, forces, moment, boundary layer characteristics, etc) are stored.
- 5- The wing and wake are discretized into number of sections. Cosine law is used to distribute the sections along the span of the wing.
- 6- Linear interpolation of the airfoils characteristics between the root and tip sections (intermediate sections), is applied.
- 7- Initial bound vortex distribution along the span of the wing is calculated from linear solution of the vortex ring method as discussed in the section 2.2. The linear solution consists of computing the influence coefficients of the bound and trailing vortices at each control point as illustrated in **Fig. 1**. Tangency boundary condition is applied at the three-quarter chord point of the wing element to solve the linear equations.
- 8- Induced angle of attack at each span wise station is then calculated from the down wash velocity at the load centre,

$$\alpha_i(y) \approx -\frac{w(y)}{V_\infty} \quad (1)$$

where  $w$  is the down wash velocity.

- 9- Effective angle of attack  $\alpha_{eff}$  is calculated by subtracting induced angle from geometric angle of attack.

$$\alpha_{eff}(y) = \alpha_g - \alpha_i(y) \quad (2)$$

10- Sectional lift coefficient can be determined from known airfoil data at effective angle of attack.

11- The new circulation distribution can be calculated by using ,Kutta-Joukowski theorem as;

$$\Gamma(y)_{2D} = \frac{cl(y) V_{\infty} c}{2} \quad (3)$$

12- The new circulation distribution is determined by the following equation;

$$\Gamma_{\text{new}} = \Gamma_{\text{old}} + D(\Gamma(y)_{2D} - \Gamma_{\text{old}}) \quad (4)$$

where D is the damping factor.

13- Step (2-11) is repeated until the difference between the old and new circulation distribution are within the given accuracy ( $1.0 \times 10^{-5}$ ).

14- The aerodynamic characteristics and boundary layer properties are calculated based on the final characteristics data obtained from 2-D airfoil characteristics at effective angle of attack and from 3-D vortex ring forces and moments.

### 3. RESULTS AND DISCUSSION

The results of the potential solution of the rectangular using are presented and discussed in the following sub sections.

#### 3.1 Validation Results

In order to verify the results with other conventional methods like vortex lattice method and experimental data obtained from published works, three test cases for accuracy are considered in the present work,

- 1- Accuracy of two-dimensional airfoil results as compared with experimental data.
- 2- Parametric considerations of the present method which includes (no. of span wise elements, damping factor, convergence tolerance).
- 3- Accuracy of nonlinear vortex ring method as compared with the published theoretical and experimental data.

The results presented in this work were programmed and executed using **Matlab 7.6** on a personal computer Dell Core i3 of (2.4) GHz. All the accuracy test cases are restricted to the rectangular or straight geometrical wing of cross-sectional airfoil NACA 0012, aspect ratio (6) and taper ratio (1).

**Fig. 3** and **4** show the aerodynamic characteristics of two-dimensional NACA 0012 airfoil at Reynolds number  $3 \times 10^6$ . The Viscous-Inviscid panel method (VIP) shows good accuracy as compared with **Abbot**, and **Von Doenhoff, 1949** experimental data except at the stalling region. The discrepancy with them may be attributed to the multiple parameters of boundary layer separation like wall roughness, pressure variation along normal direction in the separation region, position of the transition point, etc. **Fig. 3** shows a delay separation angle. **Fig. 4** shows good drag coefficient prediction because it depends on the semi-empirical equation at the tailing

edge as illustrated in **Ali, 2014**. The number of panels to represent the airfoil surface is 160 which are sufficient to give good accuracy as discussed in **Ali, 2014** with many accuracy considerations about VIP method. The pressure and shear stress distribution along the airfoil upper and lower surfaces are stored in files for next wing calculations. **Fig. 5** and **6** show Viterna results of lift and drag coefficients which extended the airfoil characteristics to high angle of attacks. Positive and negative angle of attacks are extended to  $180^\circ$  and plotted in the figures to show the behaviour of the aerodynamic characteristics at these angles. For lift coefficient in positive angles is not symmetric with negative angles due to range of exactly lift coefficient calculations ( $-10^\circ$  to  $20^\circ$ ), other this range represents the prediction results which are not bad at all. The lift coefficient at angle  $90^\circ$  is approximately zero and the drag coefficient shows the maximum value at a right angle to flow direction. These characteristics are also stored in the programs for next calculation.

Three important accuracy parameters are considered in the present method number of span wise elements, damping parameter and convergence parameter. These parameters are discussed separately to evaluate the quick and efficient solution. For the basic calculation the previous parameters are setting to the following values (20, 0.8,  $1e-4$ ) respectively.

**Fig. 7** and **8** show the effect of span wise number of elements on the lift and drag coefficients respectively for the wing geometry discussed previously at Reynolds number  $3 \times 10^6$ . The number of elements is selected 10, 20 and 40. The differences between lift coefficients for different number of elements are very small as shown in **Fig. 7**. Same results are found for total drag coefficient of the wing as illustrated in **Fig. 8**. It is clear that, when increasing the number elements of the wing, the execution time will be increased. So that, choosing 20 elements can give reasonable results and fast execution time.

The damping factor is considered in **Table 1** where the aerodynamic coefficients are investigated for the wing at  $10^\circ$  angle of attack. The damping factor is listed in table as 0.1, 0.5 and 0.8. The table shows that 0.8 damping factor is good choice for solution because it decreases the number of iteration and the execution time of the problem. No effects are noticed on the aerodynamic coefficients (lift and total drag) due to damping factor and stable solution is indicated for these ranges.

**Table 2** lists four different factors of convergence at angle of attack  $10^\circ$ . The iteration number and execution time are affected by the convergence tolerance. The iteration and time are increased as the tolerance decreased (accuracy increased). It is clear that the  $1 \times 10^{-4}$  represents a good choice to solve the problem.

The parametric consideration discussed previously shows the optimum solver conditions for rectangular wing at high angle of attack. Other consideration is required for different wing configuration. Generally, the non-linear results can be divided in to two branches. The first is the distributed coefficients (pressure, shear stress, span wise lift, transition line, etc) of the wing and the second is the aerodynamic characteristics (lift, total drag, pitching moment, centre of pressure, and aerodynamic centre) of the wing. The airfoil NACA 0012 is considered in the present analysis, which is symmetric airfoil. The results are compared with available published experimental data obtained in **Long, and Gury, 1976** for pressure distribution and lift coefficient. The wing geometric and flow characteristics are illustrated in **Table 3**.

The pressure coefficient distribution on the upper and lower surfaces at different wing sections are shown in **Fig. 9** for dynamic pressure 2.87 kPa and  $6.75^\circ$  angle of attack. As shown, the comparisons with experimental data are good for different sections of the wing. There are some discrepancy for the tip section  $y/c=0.99$  due to highly viscous tip vortex especially near

trailing edge of the wing section. Linear interpolation is used to find the pressure coefficient for the in between sections. Frictional shear stress coefficients for sections are also presented in **Fig. 10**. The frictional shear stress coefficient shows no separation along the span of the wing at this angle which indicated by a negative value of the skin friction coefficient.

**Fig. 11** shows the surface pressure distribution for different angle of attack at  $q_{\infty}=2.87$  kPa. The angle of attacks are started from  $6^{\circ}$  to  $25^{\circ}$ , separation is noticed as expected at high angle of attacks  $25^{\circ}$ . Also, the trailing edge is the first separated region on the wing a shown in the figure with red colour. The peak negative values of pressure coefficient are noticed at the leading edge of the wing. **Fig. 12** shows the skin friction drag coefficient distributed on the wing for different angle of attacks at  $q_{\infty}=2.87$  kPa. The flow separation is cleared at wing tips due to trailing vortex and at the trailing edge due to high angle of attack.

The present method lift coefficient for the wing is in good accuracy as compared with experimental data at  $q_{\infty}=2.87$  kPa obtained in **Long**, and **Gury, 1976** as shown in **Fig. 13**. The drag polar and pitching moment coefficients are shown in **Fig. 14** and **15** respectively. Also, the span wise load distribution is shown in **Fig. 16** and compared with experimental data. The results show high accuracy of about 5% error by the present method as compared with the experimental data.

#### 4. CONCLUSIONS AND RECOMMENDATIONS

The aerodynamic characteristics of rectangular wing either distributed (pressure and frictional stress coefficients) or total coefficients (lift, drag and pitching moments) are considered in the present work using a coupled method between two-dimensional characteristics of the airfoil at high angle of attack with help of Viterna method which extended the aerodynamic characteristics to high angles and that modified vortex ring method to find span wise circulation strength of the wing. Iterative method with specified accuracy is used to find the final circulation distribution along span wise direction of the wing. Two-dimensional airfoil results show good agreement with experimental data for intermediate angle of attack. To include high angles, Viterna method was used to find the aerodynamic coefficients at these angles. Parametric investigations were considered to have effective performance for the present method. The number of sections, convergence accuracy and damping factor were limited for rectangular wings. The wing of NACA 0012 airfoil section were solved and compared with published experimental data. The comparison shows excellent agreement and the accuracy reached to 5% with experiments.

The present method shows to be fast and simple to solve non-highly swept wings with different cross sectional airfoil configuration. More tests cases are required to investigate this method and more accurate solver for the two-dimensional airfoil are required like CFD to give more accurate results in 3-dimensional wing.



## 5. REFERENCES

- Abbot, I. H. and Von Doenhoff, A. E., 1949, *Theory of Wing Sections*, Dover Publications, Inc., New York, NY.
- Ali, A. H., 2014, *Aerodynamic Characteristics of Multi-Element Airfoil System with Ground Effects*, Ph.D. Thesis, Baghdad University.
- Ali, A. H., 2010, *Wake Roll-Up Behind Wings With Ground Effect*, Iraqi Journal of Mechanical and Material Engineering, Babylon University, Vol. 10, Issue 2, P.P. 181-202.
- Anderson, J. D., Corda, S., and Van Wie, D. M., 1980, *Numerical Lifting Theory Applied to Drooped Leading Edge Wings Below and Above Stall*, Journal of Aircraft, Vol. 17, No. 12, P.P. 898-904.
- Drela, M., 1989, *XFOIL, an Analysis and Design System for Low Reynolds Number Airfoils*; Massachusetts Institute of Technology, Department of Aeronautics and Astronautics, Cambridge, MA.
- Eppler, R., and Somers, D.M., 1980, *A Computer Program for the Design and Analysis of Low-Speed Airfoils*, NASA-TM-8021.
- Hess, J. L., Smith A. M. O., 1967, *Calculation of Potential Flow About Arbitrary Bodies*, Progress in Aeronautical Sciences, Vol. 8, P.P. 1-138.
- Katz, J. and Plotkin, A., 1991, *Low Speed Aerodynamics*, Cambridge University Press, Cambridge, England, UK.
- Long, P. Y., and Gury, L. S., 1976, *Pressure Distributions on a 1- By 3- Meter Semi-Span Wing at Sweep Angles From 0° to 40° in Subsonic Flow*, NASA-TN-8307.
- Mukherjee, R., Gopalarathnam, A., 2003, *An Iterative Decambering Approach for Post-Stall Prediction of Wing Characteristics Using Known Section Data*, AIAA 2003-1097.
- Piszkin, S. T., and Levinsky, E. S., 1976, *Non-Linear Lifting Line Theory for Predicting Stalling Instability on Wings of Moderate Aspect Ratio*, CASO-NSC-76-001.
- Sivells, J. C., and Neely, R. H., 1947, *Method for Calculating Wing Characteristics by Lifting Line Theory Using Non-Linear Section Lift Data*, NACA-TN-1269.
- Tangler, J. L. and Kocurek, J. D., 2005, *Wind Turbine Post-Stall Airfoil Performance Characteristics Guidelines for Blade-Element Momentum Methods*, NREL/CP-500-38456, AIAA/NREL.
- Van Dam, C. P., Vander Kam, J. C., and Paris, J. K., 2001, *Design-Oriented High-Lift Methodology for General Aviation and Civil Transport Aircraft*, Journal of Aircraft, Vol. 38, No. 6.
- de Vargas, L. A. T. and de Oliveira, P. H. I. A., 2006, *A Fast Aerodynamic Procedure for a Complete Aircraft Design Using the Know Airfoil Characteristics*, SAE Technical Paper 2006-01-2818.
- Pakalnis, E., Lasauskas, E., and Stankunas, J. 2005, *Convergence of lift force calculation of a tapered wing using non-linear section data*, Mechanika, No. 1, pp. 61 – 5.
- Spalart, P. R., 2014, *Prediction of Lift Cells for Stalling Wings by Lifting-Line Theory*, AIAA Journal, Vol. 52, pp. 1817–1821.

**NOMENCLATURE**

$c$	chord length	m
$c_l$	lift coefficient	
$D$	damping factor	
$q_\infty$	dynamic pressure $0.5\rho_\infty v_\infty^2$	Pa
$V_\infty$	free stream velocity	m/s
$w$	down wash velocity	m/s
$y$	y-axis (span wise)	m
$\alpha_{\text{eff}}$	effective angle of attack	Deg
$\alpha_g$	geometric angle of attack	Deg
$\alpha_i$	induced angle of attack	Deg
$\Gamma_{2D}$	2-dimensional circulation value	$\text{m}^2/\text{s}$
$\Gamma_{\text{new}}$	newer circulation value	$\text{m}^2/\text{s}$
$\Gamma_{\text{old}}$	previous circulation value	$\text{m}^2/\text{s}$

**Table 1.** Effect of damping factor on the numerical stability at  $\alpha= 10^\circ$ .

Damping Factor	Number of Iteration	Execution time, Sec.	Lift Coefficient	Drag Coefficient
0.1	550	3.86	0.8027	0.0448
0.5	115	0.714	0.8026	0.0447
0.8	53	0.363	0.8026	0.0447

**Table 2.** Effect of convergence tolerance on the numerical stability at  $\alpha=10^\circ$ .

Convergence Tolerance	Number of Iteration	Execution time, Sec.	Lift Coefficient	Drag Coefficient
$1 \times 10^{-3}$	44	0.394	0.8027	0.0447
$1 \times 10^{-4}$	53	0.363	0.8026	0.0447
$1 \times 10^{-5}$	66	0.461	0.8026	0.0447
$1 \times 10^{-6}$	88	0.579	0.8026	0.0447

**Table 3.** Geometric and flow field characteristics of the wing.

Wing Aspect Ratio	5.9
Sweep Angle	0
Root Airfoil Section	NACA 0012
Tip Airfoil Section	NACA 0012
Span	5.9 m
$q_\infty$	2.87 kpa
$\alpha, \beta$	$2.75^\circ, 0^\circ$

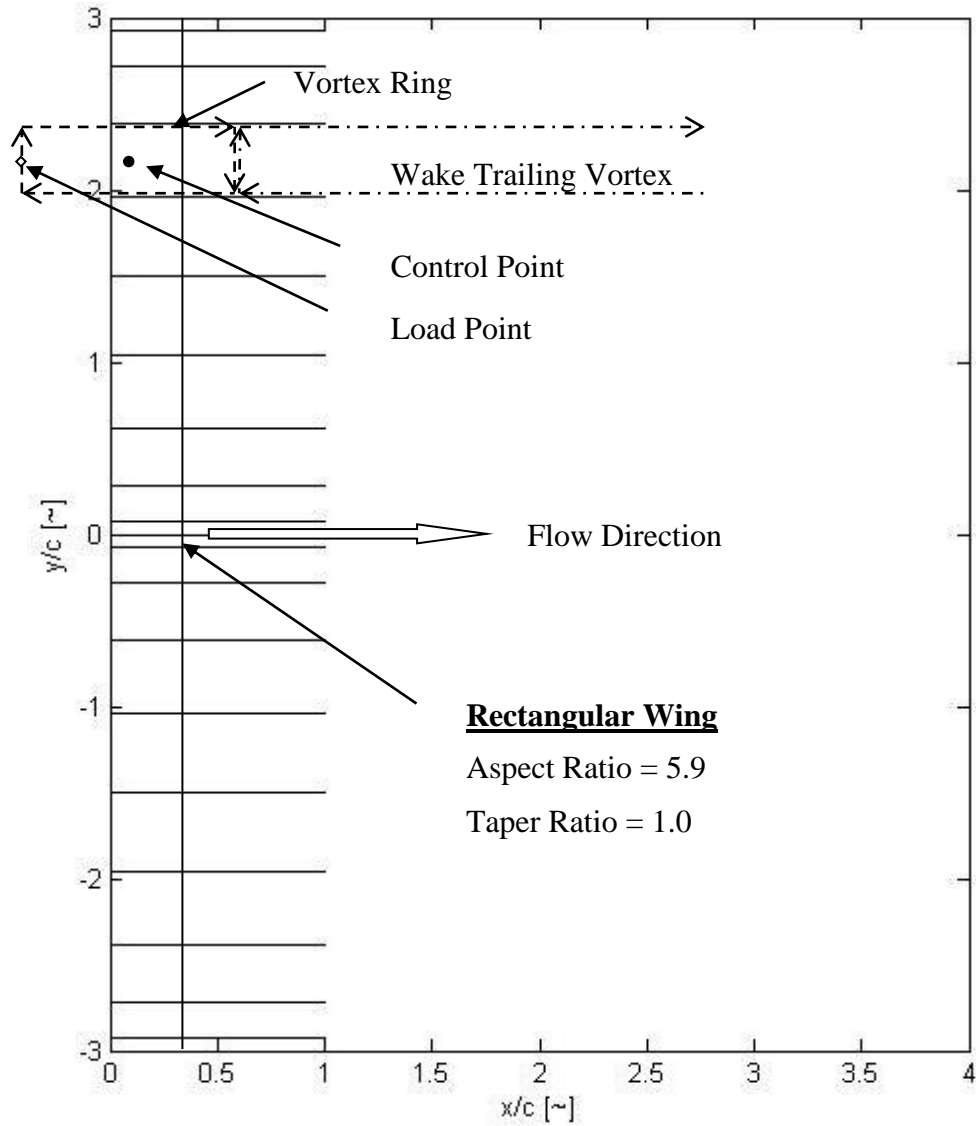


**Figure 1.** Discretization of the vortex ring method for rectangular wing (top view).

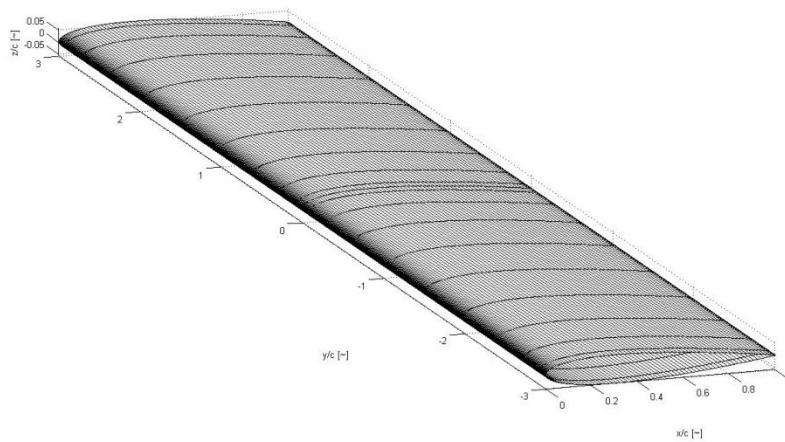


**Figure 2.** Two and three-dimensional discretization conjunction for a rectangular wing.

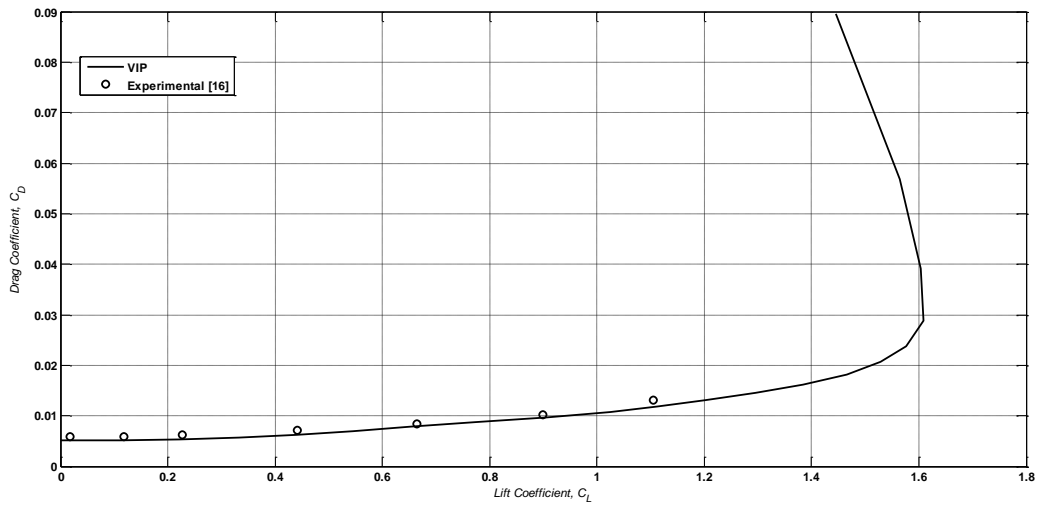


Figure 3. Two-dimensional lift coefficient for NACA 0012 airfoil at  $Re=3 \times 10^6$ .

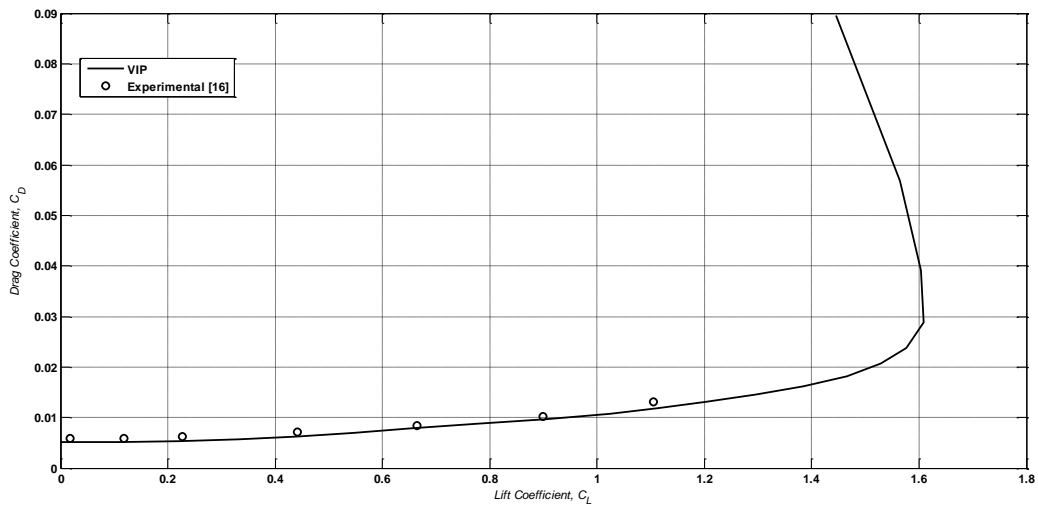


Figure 4. Two-dimensional drag coefficient for NACA 0012 airfoil at  $Re=3 \times 10^6$ .

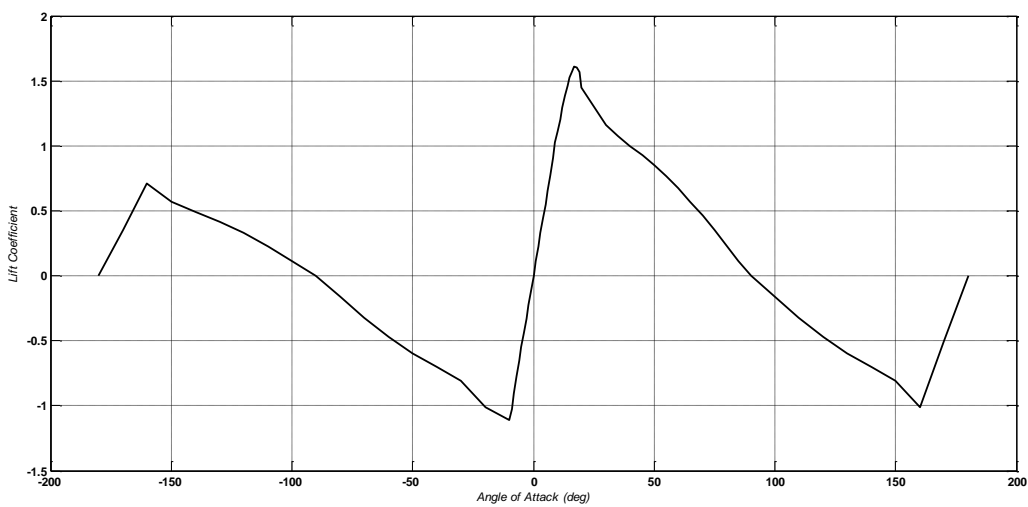


Figure 5. Viterna method to find lift coefficient of NACA 0012 airfoil at high AoA.

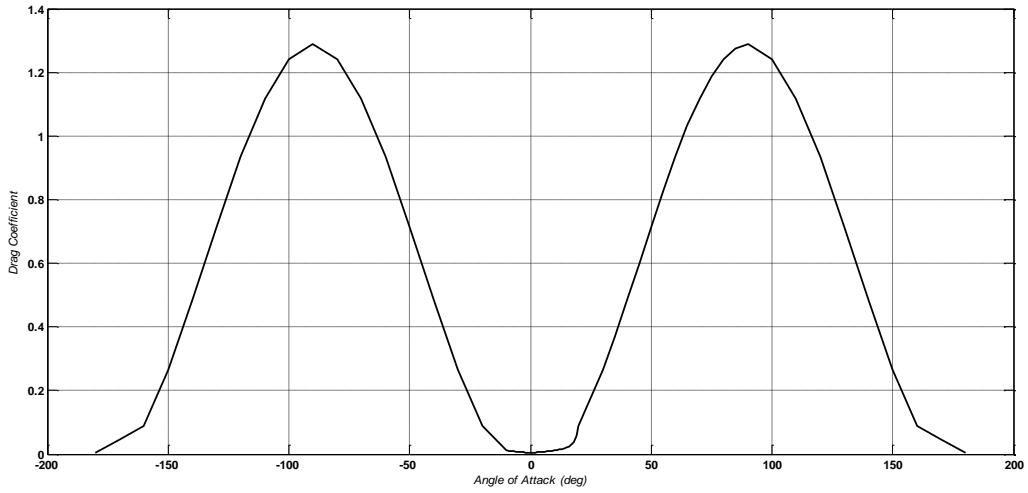


Figure 6. Viterna method to find lift coefficient of NACA 0012 airfoil at high AoA.

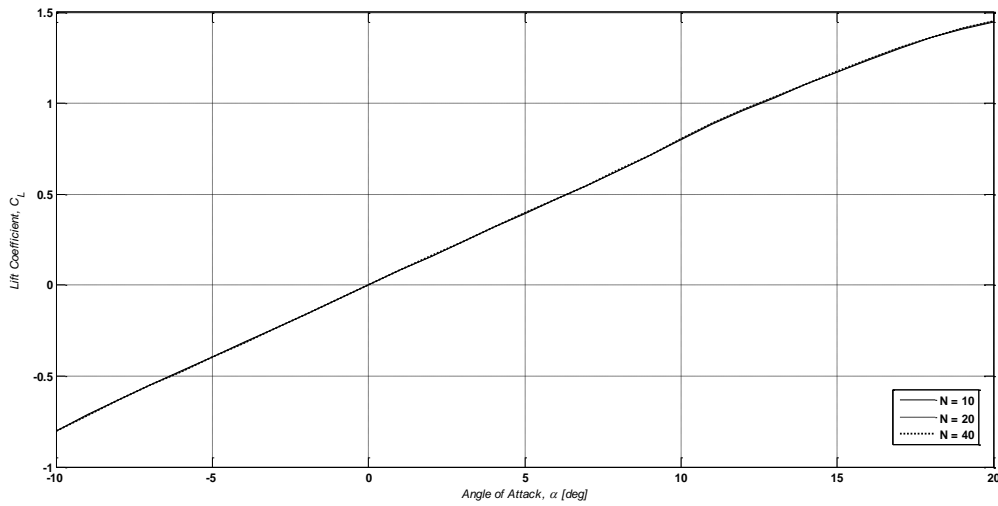


Figure 7. Lift coefficient of the wing affected by number of sections for  $Re=3 \times 10^6$ .

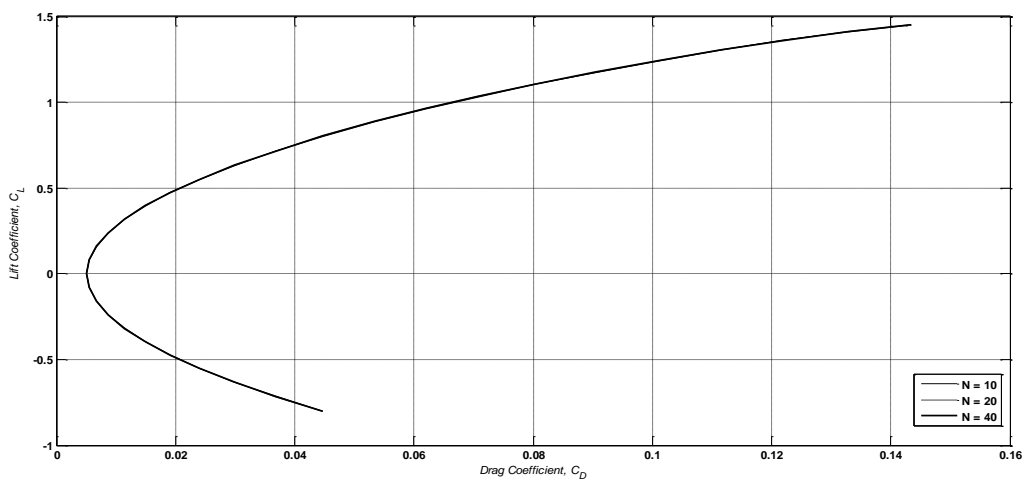


Figure 8. Lift coefficient of the wing affected by number of sections for  $Re=3 \times 10^6$ .

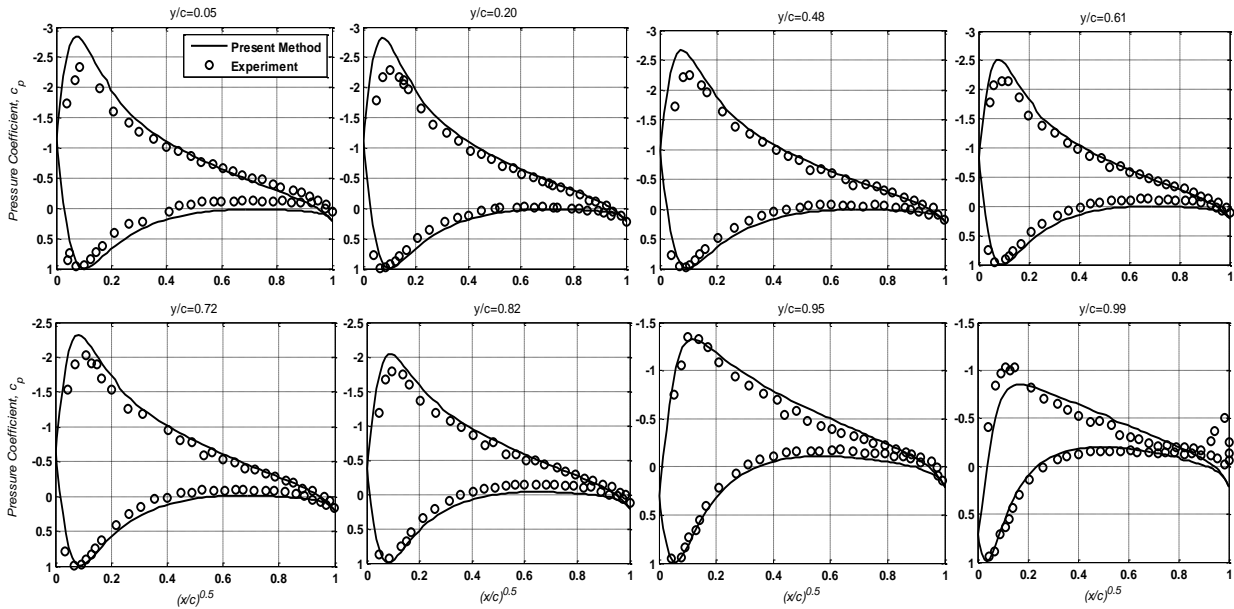


Figure 9. Pressure Distribution for different sections of the wing at  $\alpha=6.75^\circ$  and  $q_\infty=2.87$  kPa where – theory & o experiment.

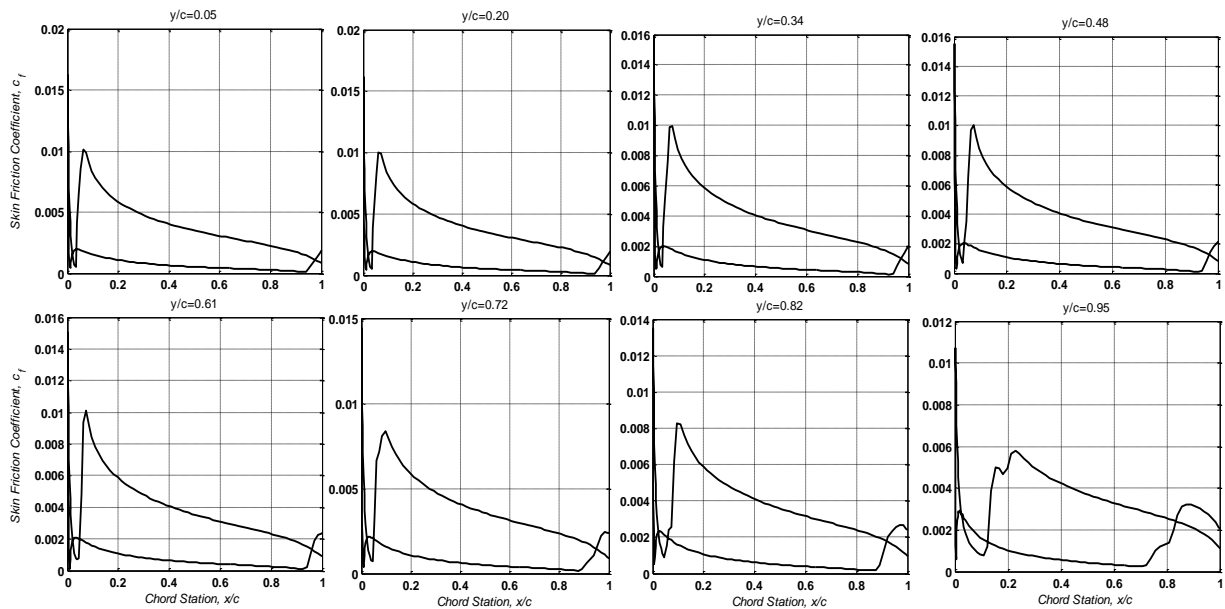


Figure 10. Frictional shear stress distribution for different sections of the wing at  $\alpha=6.75^\circ$  and  $q_\infty=2.87$  kPa where – theory & o experiment.

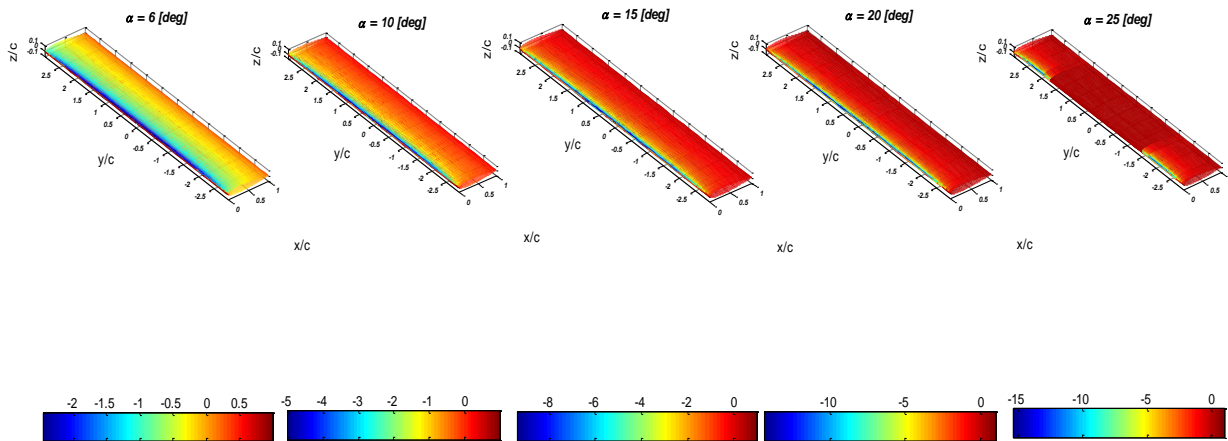


Figure 11. Wing surface pressure coefficient distribution at  $q_{\infty}=2.87$  kPa.

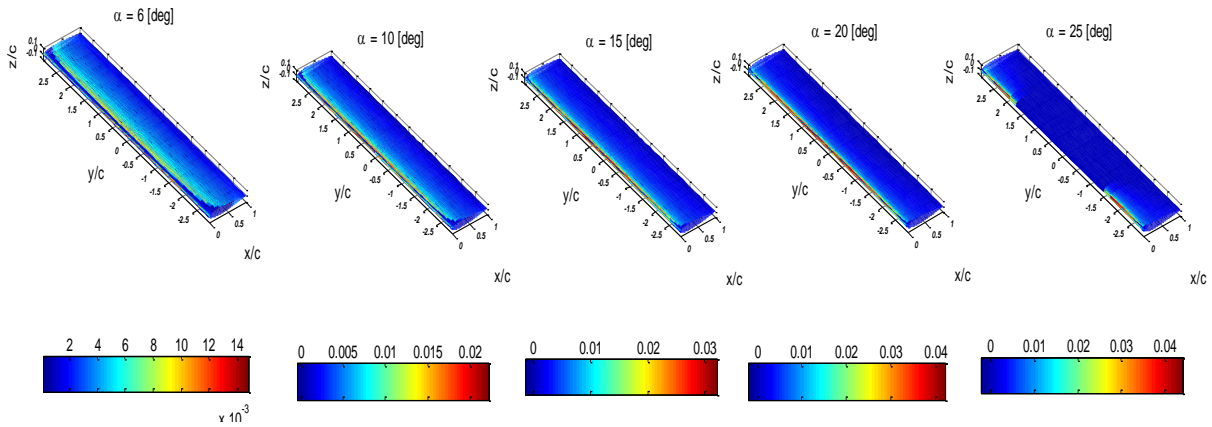


Figure 12. Wing skin friction coefficient distribution at  $q_{\infty}=2.87$  kPa.

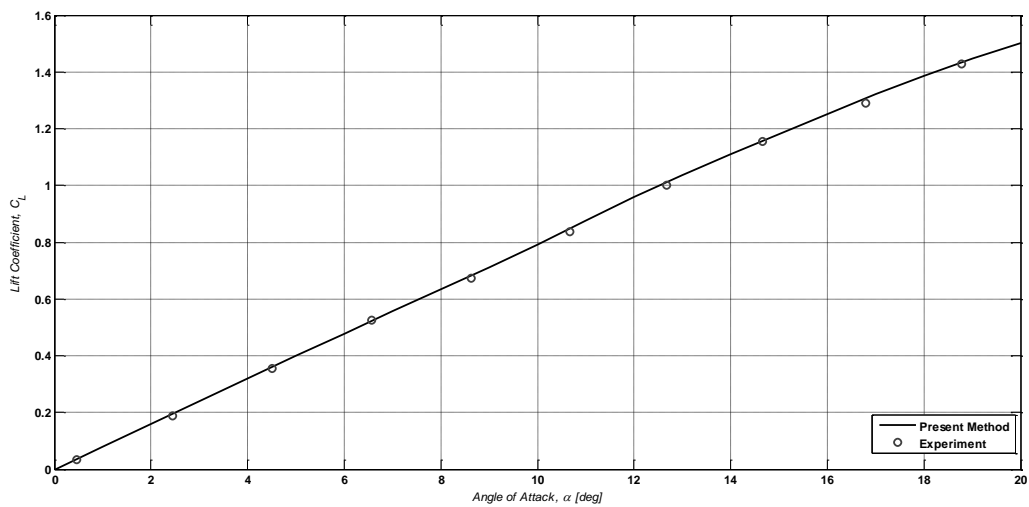


Figure 13. Lift coefficient for wing of NACA 0012 airfoil section at  $q_{\infty}=2.87$  kPa.

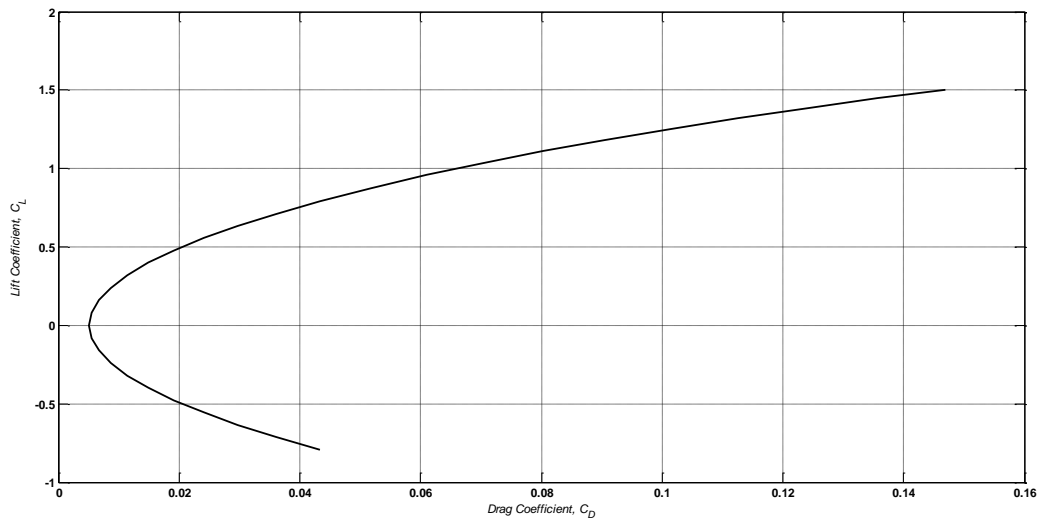


Figure 14. Drag polar for wing of NACA 0012 airfoil section at  $q_{\infty}=2.87$  kPa.

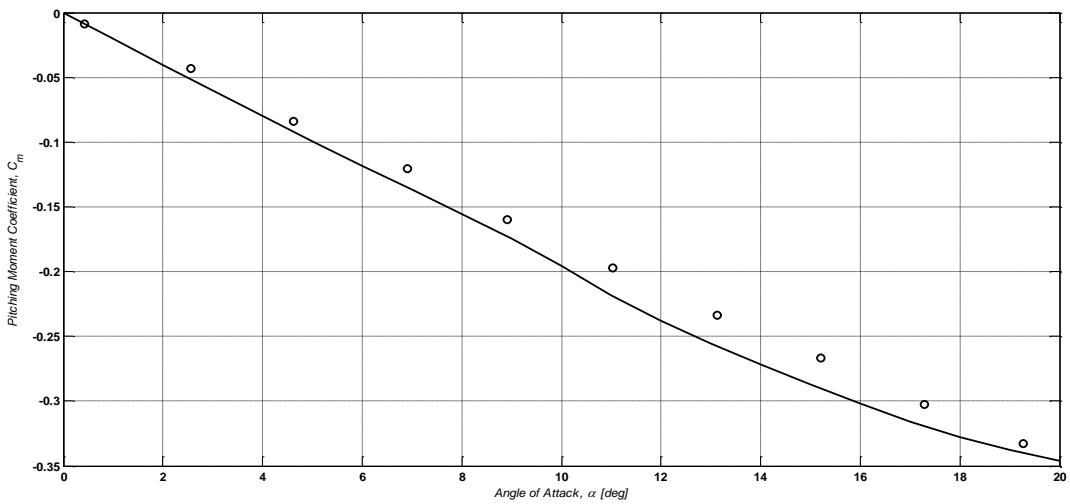


Figure 15. Pitching moment coefficient for wing of NACA 0012 airfoil section at  $q_{\infty}=2.87$  kPa.

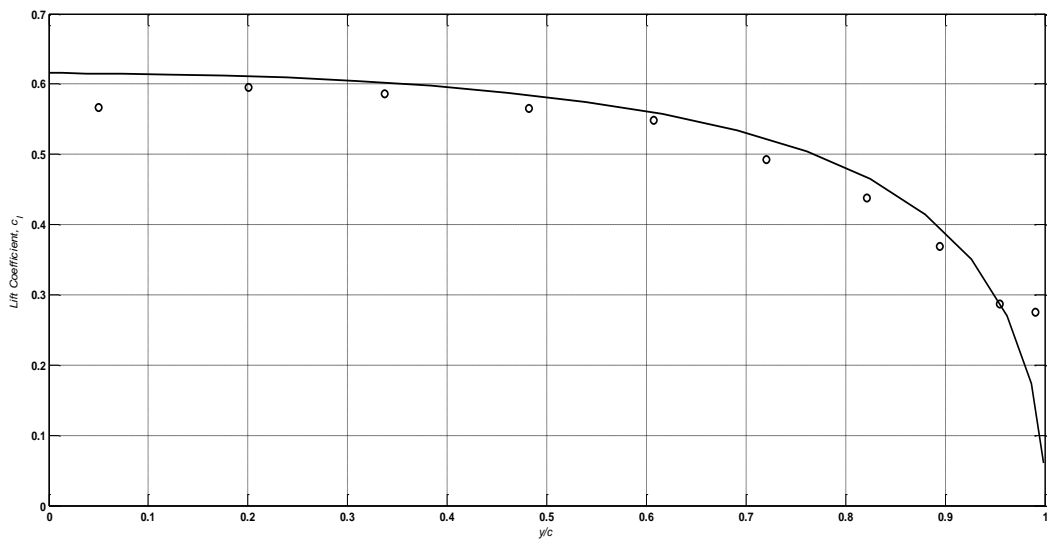


Figure 16. Span wise lift coefficient distribution of the wing at  $\alpha=6.75^\circ$  and  $q_{\infty}=2.87$  kPa.